Lasers in Manufacturing and Materials Processing (2023) 10:471–484
https://doi.org/10.1007/s40516-023-00220-x

RESEARCH

# Deformed Ternary Phosphides III-P for Efficient Light Control in Optoelectronic Applications

**A. Tarbi[1] · T. Chtouki[2] · M. A. Sellam[1] · A. Benahmed[3] · Y. El kouari[1] · H. Erguig[2] · A. Migalska-Zalas[4] · I. Goncharova[5,6] · S. Taboukhat[6] · M. Tlemçani[7,8]**

Accepted: 28 June 2023 / Published online: 3 July 2023


## Abstract

In this study, we simulated the response of ternary phosphide materials subjected to a strain due to the lattice mismatch; the study was made by varying the concentration of phosphorus P(x). The impact of strain could provide additional opportunities to obtain the desired optoelectronic properties. This study focused on the bandgap energy, absorption coefficient, refractive index, and dielectric constant of the GaAsP and GaSbP ternary alloys grown on GaAs substrate. Shear deformation makes it possible to lift the degeneration of the valence band of the strained layers, which leads to the appearance of two sub-bands associated with light holes (lh) and heavy holes (hh). The displacement of the sub-bands generates a new and wide range of refractive indices. In the case of GaAsP/GaAs, the incorporation of P(x) causes a linear reduction in the refractive index from 3.01 to 2.59. In contrast, in GaSbP/GaAs, the refractive index initially increases, reaching a maximum of 3.24 at x = 28% phosphorus composition. However, with further increase in the phosphorus content, the refractive index decreases again and eventually converges to 2.59. The high refractive index contrast, particularly for deformed GaSbP/GaAs, can be utilized to optimize the design of optical sensors based on optical waveguides.

**Keywords** Ternary phosphides · Optoelectronics · Optical sensors

## Introduction

The possibility of changing the refractive index of a material can be used for the design of step-index structures, which will aid in help the design new applications. The band engineering of III-P materials is of interest [1–3], which can create different and modulable electromagnetic characteristics by introducing the lattice detuning effect and by varying the concentration of phosphorus [4]. The lattice mismatch leads rise to deformation of the GaAsP and GaSbP materials on

Extended author information available on the last page of the article

the GaAs substrate. If this lattice mismatch is relatively small (ε ~ 2%), the atoms of the ternary place themselves in a low-energy configuration, and the bonds are strained such that the lattice parameter of the ternary corresponds to that of the substrate [5]. As the layers are added, the energy stored in the bonds becomes important [6], which generates plastic deformation due to the rupture of bonds, consequently, there will be an appearance of defects [7]. The calculation of the critical thickness makes it possible to estimate the type of deformation existing in the ternary. The change in phosphorus concentration, and lattice mismatch can help in designing an optical waveguide, which is usually made of a transparent dielectric guiding layer epitaxied between two transparent dielectric media of lower refractive index. In this work, we want to highlight the variation of opto-electronic properties such as the refractive index [8], the dielectric constant, and the absorption coefficient of ternary GaAsP and GaSbP on the GaAs substrate, as a function of the deformation due to the detuning of the lattice, controlled by the concentration of P(x), the impact of temperature, and pressure [9].

## Theoretical Approach

The strain resulting from the stress modifies the internal potential energy created by Coulomb forces [10]; therefore, it also modifies the bandgap energy of ternary GaAsP and GaSbP on the GaAs substrate, as shown in Fig. 1. The strain potentials used in the study are listed in Table 1.

Two distinct strains affect the energy position of the bands: hydrostatic strain affects the conduction and the valence bands and shear strain, which makes it possible to remove the degeneracy of the levels of the valence band. Consequently, two valence bands appear: the first is associated with light holes (lh) and the second is associated with heavy holes (hh) [16, 17]. The lattice mismatch is given by the following equations [18, 19].

$$\varepsilon_{\parallel} = \frac{a_{sub} - a_t}{a_t} \tag{1}$$

$$\varepsilon_{\perp} = -2 \times \frac{C_{12}}{C_{11}} \times \varepsilon_{\parallel} \tag{2}$$

$a_{sub}$ and $a_t$ are the lattice parameters of the GaAs substrate and ternary substrates, respectively, and $C_{11}$ and $C_{12}$ are elastic coefficients that depend on the material [20].

The bandgap energy affected by the compressive and tensile strains is given respectively by the following equations:

$$E_{ghh} = E_g^{\Gamma} + \Delta E_c^{hyd} - \Delta E_{v,avg}^{hyd} - \Delta E_{hh}^{sh} \tag{3}$$

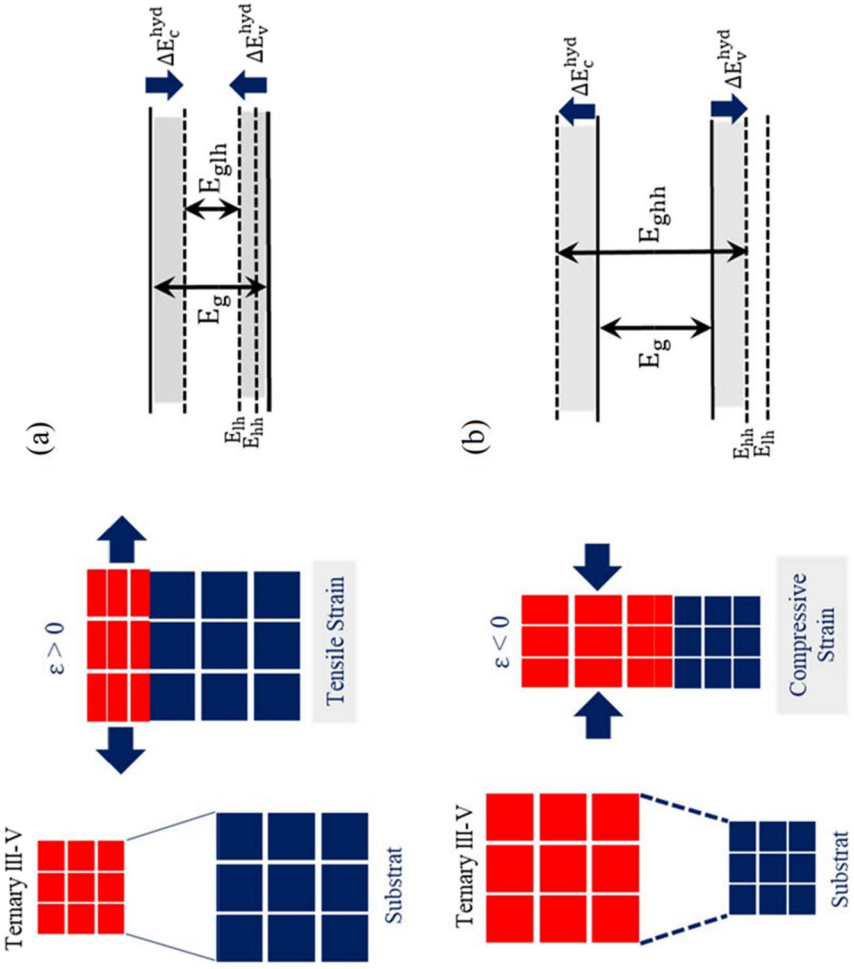


**Fig. 1** Two-dimensional representation of the material under strain and the effect of strain on the energy diagram: **a** compressive strain and **b** tensile strain

**Table1** Parameters of binaries constituting the GaAsP and GaSbP ternary alloys [4, 11–15]

| | GaAs | GaP | GaSb |
|---|---|---|---|
| a (Å) | 5.6536 | 5.4512 | 6.09593 |
| $a_c$ (eV) | –7.17 | –8.2 | –7.5 |
| $a_v$ (eV) | 1.16 | 1.7 | –0.8 |
| b (eV) | –2 | –1.6 | –2 |
| $C_{11}$ (GPa) | 1221 | 1405 | 884.2 |
| $C_{12}$ (GPa) | 566 | 620.3 | 402.6 |

$$E_{glh} = E_g^{\Gamma} + \Delta E_c^{hyd} - \Delta E_{v,avg}^{hyd} - \Delta E_{lh}^{sh} \tag{4}$$

$\Delta E_c^{hyd}$ and $\Delta E_{v,avg}^{hyd}$ represent the changes in band energy due to hydrostatic deformation, and $\Delta E_{hh}^{sh}$ is the change in band energy due to shear.

Eg(GaAsP) and Eg(GaSbP) are the bandgap energies of $GaAs_{1-x}P_x$ and $GaSb_{1-x}P_x$, respectively, through the high-symmetry point Γ of the Brillouin zone, as given by the following equations [21]:

$$E_g^{\Gamma}(GaAs_{1-x}P_x) = 1.42 + 1.16x + 0.2x^2 \tag{5}$$

$$E_g^{\Gamma}(GaSb_{1-x}P_x) = 0.73 - 0.65x + 2.7x^2 \tag{6}$$

Balance theories have been used to model the critical thickness, and Matthews and Blackslee [22] describes it using the following equation:

$$L_c = \frac{a_{GaAs}}{2\sqrt{2}\pi\varepsilon\beta}\frac{1-0.25\sigma}{1-\sigma}\ln\left(\frac{L_c\sqrt{2}}{a_{GaAs}} + 1\right) \tag{7}$$

The Poisson's ratio σ is given by the following expression:

$$\sigma = \frac{C_{12}(GaAs)}{C_{11}(GaAs) + C_{12}(GaAs)} \tag{8}$$

where $C_{11}$(GaAs) and $C_{12}$ (GaAs) are the elastic coefficients of the GaAs substrate and β is a coefficient that depends on the structure of the material.

The absorption coefficient α enables the description of the response of a material to photon excitation. The electrons of the valence band absorb photons and jump to the conduction band, and the expression for the absorption coefficient in the case of a direct band is [23]:

$$\alpha(E) = \frac{A}{E}\left(E - E_g\right)^{1/2} \tag{9}$$

where E = hν, h is Planck's constant, and ν is frequency.

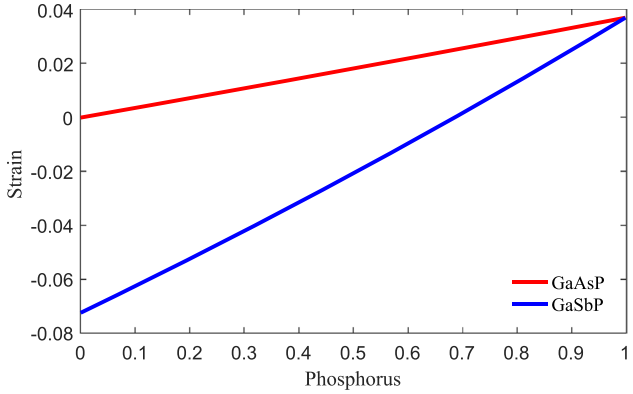


**Fig. 2** Variation in deformation according to phosphorus concentrationfor the GaAsP and GaSbP ternary alloys on GaAs

The refractive index has a direct relationship with the bandgap energy of the deformed material and can be estimated using the empirical Moss method [24]:

$$n = \sqrt[1/4]{\frac{h'}{E_g}} \tag{10}$$

h' is a constant equal to 108 eV. The high-frequency optical dielectric constant is expressed as:

$$\varepsilon_\infty = n^2 \tag{11}$$

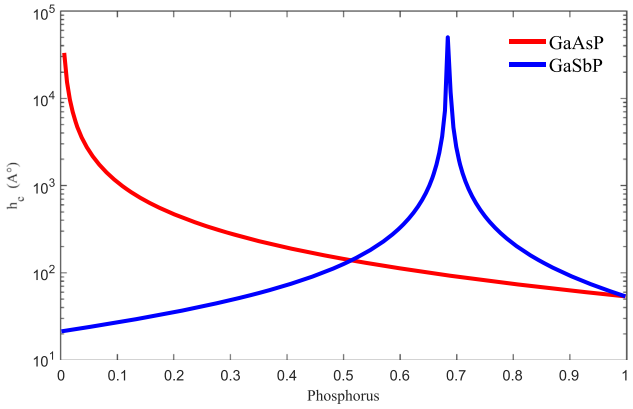


**Fig. 3** Variation of critical thickness as a function of phosphorus concentration for GaAsP and GaSbP ternary alloys on a GaAs substrate

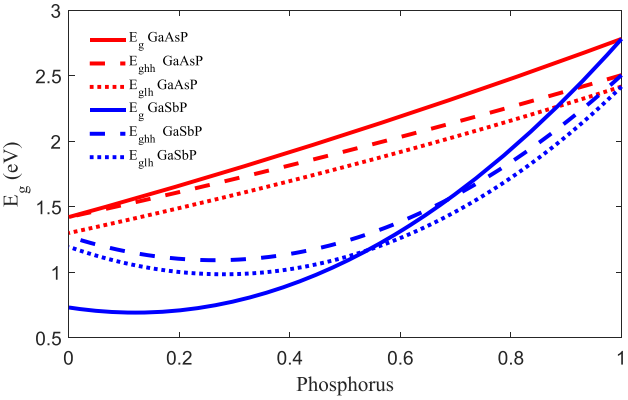


**Fig. 4** Representation of bandgap energies through the high-symmetry point Γ of the Brillouin zone of deformed and undeformed GaAsP and GaSbP ternary structures on the GaAs substrate as a function of P(x)

## Results and Discussion

Figure 2 shows the variation in strain ε as a function of P(x). The strain ε is always positive for the GaAsP/GaAs ternary material because the lattice constant can only get smaller compared with GaAs when the P(x) is added, and it increases with increasing P(x) from 0 to 3.7%. It should be noted that the GaAsP material was lattice-matched to GaAs at 0%. For the GaSbP/GaAs ternary material, the strain is positive when P(x) exceeds 69% and it increases with increasing P(x) from 0 to 3.7%, indicating that the lattice constant of the GaAs substrate is larger than that of the ternary material; resulting in the appearance of extensive strain. Removing P(x) atoms increases the lattice parameter of the GaSbP ternary, resulting in a negative strain and leading to compressive strain, which increases up to |ε|=7.3%. GaSbP is lattice-matched to GaAs at approximately 70%.

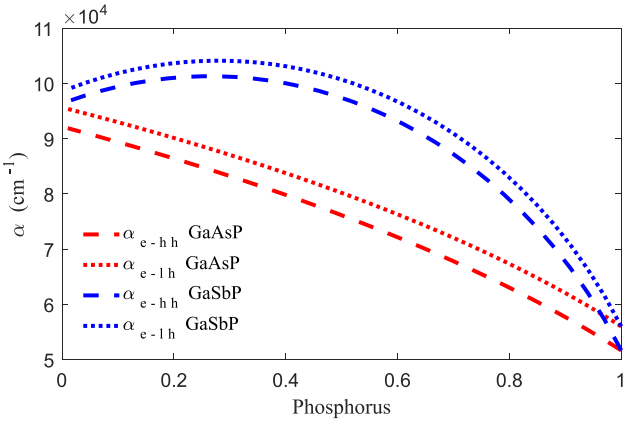


**Fig. 5** Variation in the absorption coefficients of GaAsP and GaSbP ternary alloys elaborated on the GaAs substrate subjected to deformation as a function of P(x) excited by energy E = 3 eV

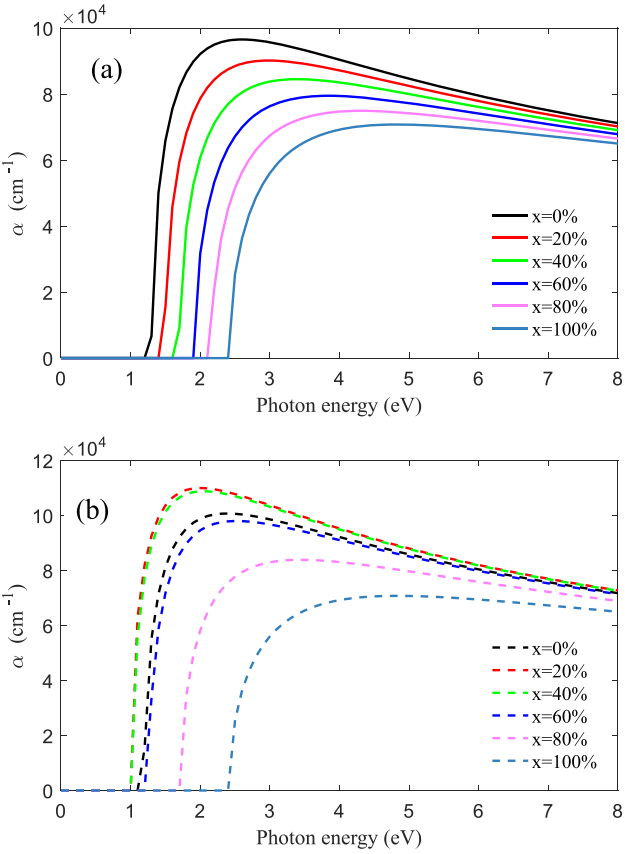


**Fig. 6** Variation in the absorption coefficient $\alpha_{e\text{-}lh}$ for (**a**) GaAsP and (**b**) GaSbP ternary alloys on GaAs under deformation, as a function of photon energy

Figure 3 illustrates a comparison of the critical thickness between GaAsP and GaSbP materials on GaAs substrate as a function of the P(x) composition, it takes maximum values when the materials are in agreement with their substrates, the highest critical thickness is verified by the GaSbP/GaAs ternary. For both GaAsP and GaSbP ternary alloys elaborated on the GaAs substrate, the critical thickness decreased with increasing P(x) in the area of tensile strain (i.e., for compositions where $P > 0\%$ in GaAsP and $P > 69\%$ in GaSbP). For ternary GaSbP/GaAs, the critical thickness increased with increasing P(x) up to $x = 69\%$ because of the decreasing compressive strain over this composition range. The GaSb binary is likely to create irreversible deformations because of its instability, on the other hand, the GaAs binary is more stable.

Figure 4 shows the variation in the bandgap energy $E_g$ of the undeformed material and material subjected to a constraint ($E_{glh}$, $E_{ghh}$). With respect to the GaAsP/GaAs ternary material, the increase in P(x) led to a linear increase in the bandgap energy and a shift between the energy $E_g$ and $E_{glh}$ from the degenerate point

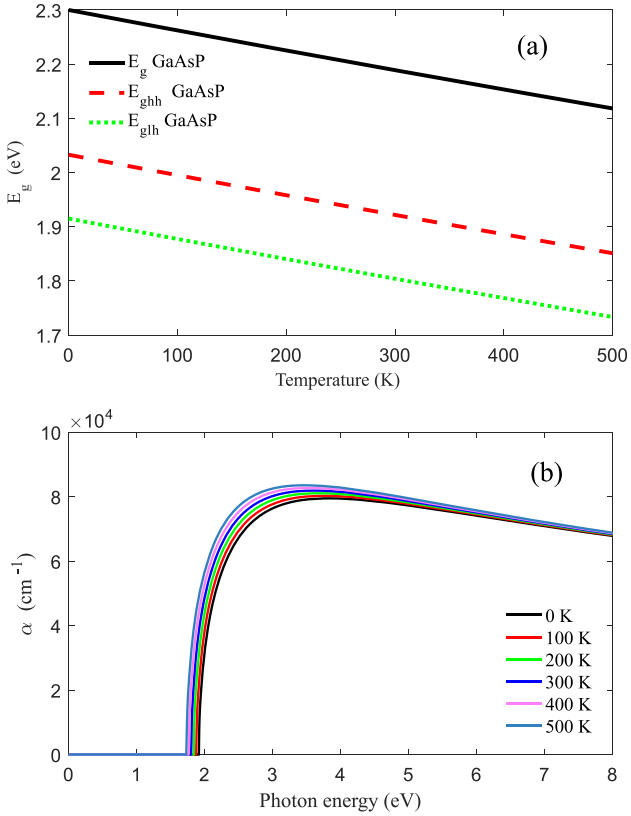


**Fig. 7** Impact of temperature on: **a** the bandgap energies through the high-symmetry point Γ of the Brillouin zone, and **b** the absorption coefficient $\alpha_{e\text{-}lh}$ for the $GaAs_{0.5}P_{0.5}$ ternary alloy on GaAs under deformation, as a function of photon energy

(x = 0%). For ternary GaSbP/GaAs, the energy was parabolic. When P(x) exceeds 69%, the $E_{glh}$ energy is considered to be the smallest, and it is responsible for the electronic transport. When x < 69%, the energy $E_{ghh}$ is the highest, and it is responsible for electronic transport in this zone. The point that corresponds to the concentration (x = 69%) represents the point of degeneracy of the valence energy levels, this is due to lack of strain, because this is where GaSbP is lattice-matched to the GaAs substrate.

Figure 5 illustrates the variation in absorption coefficient α of the GaAsP and GaSbP ternary alloys on GaAs as a function of P(x). The absorption coefficient of the GaSbP/GaAs ternary material is larger than that of the GaAsP/GaAs ternary material. For GaAsP/GaAs, the absorption coefficient decreased with increasing P (x), whereas for GaSbP/GaAs, the absorption coefficient decreased with increasing P (x) until a peak corresponded to x = 28% and then decreased with increasing P(x). These results can be explained by the variation in bandgap energy of the material.

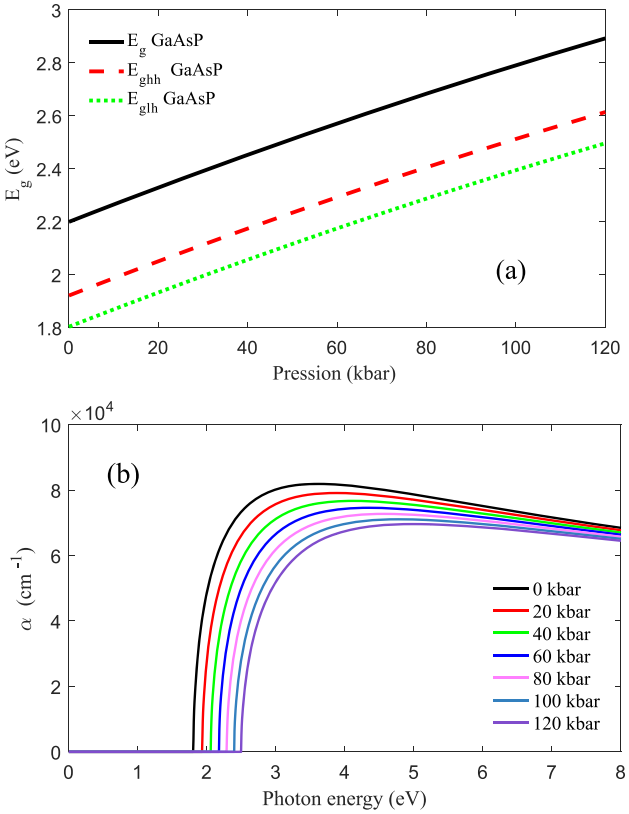


**Fig. 8** Impact of pressure on: **a** the bandgap energies through the high-symmetry point Γ of the Brillouin zone, and **b** the absorption coefficient $\alpha_{e\text{-}lh}$ for $GaAs_{0.5}P_{0.5}$ ternary alloy on GaAs under deformation, as a function of photon energy

Figure 6 shows the absorption coefficient of the GaAsP and GaSbP ternary structures on GaAs as a function of photon energy E. Peaks in the absorption coefficient achieved by the GaAsP/GaAs ternary structure increase with the decrease in P(x), while the peaks achieved by the GaSbP/GaAs ternary structure increase with the increase in P(x) up to x = 28%, and then decrease with further increases in P(x). This is due to the fact that the absorption coefficient is inversely proportional to the bandgap energy.

Figure 7b illustrates the variation in the absorption coefficient in the $GaAs_{0.5}P_{0.5}$ ternary on GaAs as a function of photon energy, while also considering the temperature range from 0 to 500 K in increments of 100 K. The temperature increased the peaks of the curves and decreased the threshold excitation energy, which can be explained by the decrease in the bandgap energy $E_{glh}$ with increasing temperature, as shown in the Fig. 7a.

Figure 8b shows the variation in the absorption coefficient of the $GaAs_{0.5}P_{0.5}$ ternary as a function of photon energy and by varying the pressure from 0 to 120

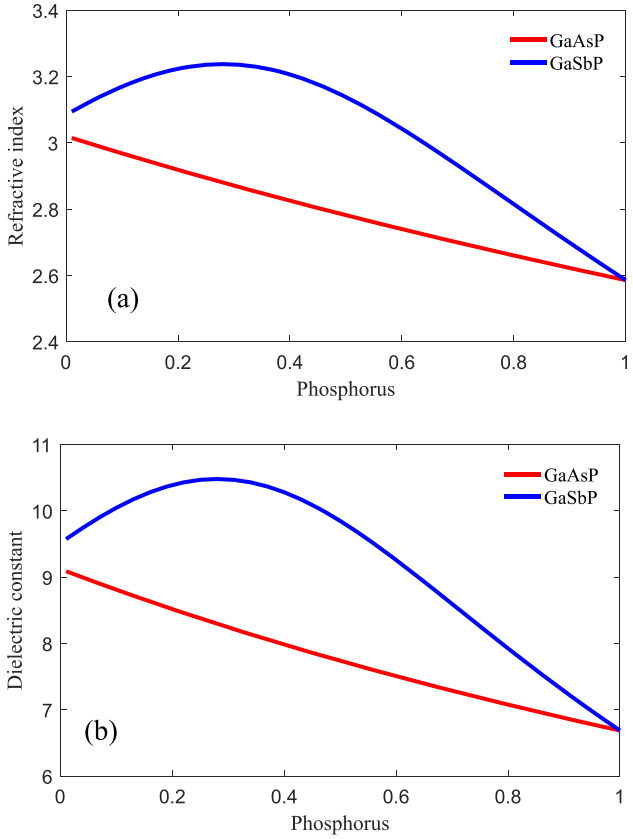


**Fig. 9** Variation of (**a**) the refractive index and (**b**) dielectric constant, corresponding to the e-lh transition, for GaAsP and GaSbP ternary alloys on GaAs under deformation, as a function of P (x)

kbar in steps of 20 kbar. Increasing the pressure decreased the absorption coefficient and the sensitivity to excitation. These results can be explained by the increase in bandgap energy $E_{glh}$ (Fig. 8a). We can conclude that the impact of pressure applied to the deformed material [0 kbar -120 kbar] is very high compared to the impact of temperature [0 K- 500 K].

Figure 9 illustrates the variation in the refractive index and dielectric constant as a function of P(x). For GaAsP on GaAs, these parameters decrease almost linearly with increasing P(x). For GaSbP/GaAs, increases with an increase in P(x), reaching a maximum at x = 28%, and then they decreased with an excess of P(x). This deformation makes it possible to widen the range of the refractive index, which is beneficial in the design of optical sensors.

Figure 10 shows the variation in the dielectric constant with the temperature (Fig. 9a) and pressure (Fig. 9b), it increased linearly with increasing temperature anddecreased with increasing pressure in a parabolic manner.

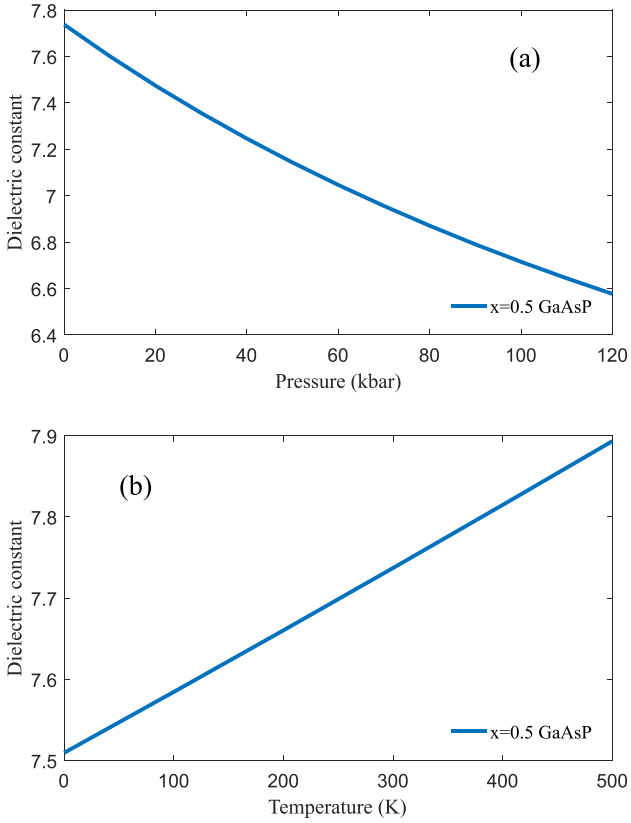


**Fig. 10** Variation in the refractive index corresponding to the e-lh transitions of the $GaAs_{0.5}P_{0.5}$ ternary on GaAs subjected to (**a**) a temperature range of 0 and 500 K, and (**b**) pressures ranging from 0 to 120 kbar

## Conclusion

Summarizing the results, we conclude that the lattice mismatch between the III-P ternary and GaAs substrates affects their optoelectronic properties. The deformation is positive in the ternary ($GaAs_{1-x}P_x$ with $0\% < x < 100\%$) and ($GaSb_{1-x}P_x$ with $x > 69\%$); it increases with the increase in P(x), the ternary alloys undergo extensive strain, and the bandgap energy narrows, which promotes the passage of electrons from the valence band to the conduction band, leading to an increase in the absorption coefficient. The refractive index and dielectric constant decreased with increase in P(x). However, an increase in Sb concentration ($> 30\%$) leads to compressive strain, the bandgap energy becomes wide, and we noticed a nonlinear evolution of the optoelectronic parameters of the $GaSb_{1-x}P_x$ ternary material with $x < 69\%$. Thus, the impact of strain could provide additional opportunities to obtain desired optoelectronic properties. The range of refractive index widens, particularly for ternary GaSbP/GaAs, which aids in the design of optical waveguides.

**Acknowledgements** The authors would like to thanks Professor Bouchta SAHRAOUI from University of Angers, France for his helpful discussions.

**Authors Contribution** A. Tarbi: Conceptualization, Writing – original draft.
T. Chtouki: Writing – review & editing.
M. A. Sellam: Writing – review & editing.
A. Benahmed: Writing – review & editing.
Y. El kouari: Writing – review & editing.
H. Erguig: Writing – review & editing.
A. Migalska-Zalas: Writing – review & editing.
I. Goncharova: Writing – review & editing.
S. Taboukhat: Writing – review & editing.
M. Tlemçani: Writing – review & editing.
All authors have read and agreed to the published revised version of the manuscript.

**Data Availability** All data generated or analyzed during this study are included in this published article.

## Declarations

**Ethical Approval** Not applicable.

**Conflict of Interest** I declare that no conflict of interest exists.

**Declaration of Interest** All authors have participated in (a) conception and design, or analysis and interpretation of the data; (b) drafting the article or revising it critically for important intellectual content; and (c) approval of the final version.

This manuscript has not been submitted to, nor is under review at, another journal or other publishing venue.
The authors have no affiliation with any organization with a direct or indirect financial interest in the subject matter discussed in the manuscript. The following authors have affiliations with organizations with direct or indirect financial interest in the subject matter discussed in the manuscript.
No financial support.

**Competing Interests** The authors declare no competing interests.

## References

1. Tarbi, A., Atmani, E.H., Sellam, M.A., Lougdali, M., El Kouari, Y., Migalska-Zalas, A.: Theoretical diagnostic and prediction of physical properties of quaternary InGaAsP compound using artificial neural networks optimized by the Levenberg Maquardt algorithm. Opt. Quant. Electron. **50**(7), 1–21 (2018)
2. Adachi, S.: Physical properties of III-V semiconductor compounds. Wiley (1992)
3. Tarbi, A., Chtouki, T., Benahmed, A., Sellam, M.A., Elkouari, Y., Erguig, H., Aissat, A.: Optimization by simulation for photovoltaic applications of the quaternary semiconductor InGaAsP epitaxed on InP substrate. Opt. Quant. Electron. **53**(3), 1–13 (2021)
4. Vurgaftman, I., Meyer, J.Á., Ram-Mohan, L.Á.: Band parameters for III–V compound semiconductors and their alloys. J. Appl. Phys. **89**(11), 5815–5875 (2001)
5. Mori, M.J.: Lattice mismatched epitaxy of heterostructures for non-nitride green light emitting devices. Doctor of Philosophy in Electronic Materials, Department of Materials Science and Engineering, Massachusetts Institute of Technology, 165 pages (2008)
6. Kapustianyk, V., Turko, B., Kostruba, A., Sofiani, Z., Derkowska, B., Dabos-Seignon, S., ... Sahraoui, B.:. Influence of size effect and sputtering conditions on the crystallinity and optical properties of ZnO thin films. Opt. Commun. **269**(2), 346–350 (2007)

7. Matthews, J.W., Blakeslee, A.E.: Defects in epitaxial multilayers: I. Misfit dislocations. J. Cryst. Growth **27**, 118–125 (1974)
8. Rabah, M., Abbar, B., Al-Douri, Y., Bouhafs, B., Sahraoui, B.: Calculation of structural, optical and electronic properties of ZnS, ZnSe, MgS, MgSe and their quaternary alloy $Mg_{1-x}Zn_xS_ySe_{1-y}$. Mater. Sci. Eng., B **100**(2), 163–171 (2003)
9. Degheidy, A.R., Elabsy, A.S., Elkenany, E.B.: Optoelectronic properties of GaAs1−xPx alloys under the influence of temperature and pressure. Superlattices Microstruct. **52**(2), 336–348 (2012)
10. Gélinas, G.: Comprendre et maîtriser le passage de type I à type II de puits quantiques d'$In_{(x)}$ $Ga_{(1-x)}$ $As_{(y)}$ $Sb_{(1-y)}$ sur substrat de GaSb. Department of Physics, Faculty Arts and Sciences, University of Montreal, 282 pages (2016)
11. Tarbi, A., Chtouki, T., Elkouari, Y., Erguig, H., Migalska-Zalas, A., Aissat, A.: Bandgap energy modeling of the deformed ternary GaAs1-uNu by artificial neural networks. Heliyon **8**(8), e10212 (2022)
12. Aissat, A., Alshehri, B., Nacer, S., Vilcot, J.P.: Theoretical investigation of GaAsNBi/GaAs materials for optoelectronic applications. Mater. Sci. Semicond. Process. **31**, 568–572 (2015)
13. Tarbi, A., Chtouki, T., Sellam, M.A., Elkouari, Y., Erguig, H., Migalska-Zalas, A.: Predicting the bandgap energy of distorted $GaSb_xAs_{1-x}$ and InSbxAs1-x using design of experiment (DoE) and artificial intelligence (AI): A comparative study. J. Phys. Chem. Solids **175**, 111180 (2023)
14 Aissat, A., Bestam, R., Vilcot, J.P.: Modeling and simulation of $Al_xGa_yIn_{1-x-y}As$/InP quaternary structure for photovoltaic. Int. J. Hydrogen Energy **39**(27), 15287–15291 (2014)
15. Tarbi, A., Chtouki, T., Erguig, H., Migalska-Zalas, A., Aissat, A.: Modeling and optimization of Sb and N resonance states effect on the band structure of mismatched III-NV alloys using artificial neural networks. Mater. Sci. Eng., B **290**, 116312 (2023)
16. Krijn, M.P.C.M.: Heterojunction band offsets and effective masses in III-V quaternary alloys. Semicond. Sci. Technol. **6**(1), 27 (1991)
17. O'Reilly, E.P.: Valence band engineering in strained-layer structures. Semicond. Sci. Technol. **4**(3), 121 (1989)
18. Van de Walle, C.G.: Band lineups and deformation potentials in the model-solid theory. Phys. Rev. B **39**(3), 1871 (1989)
19. Tarbi, A., Chtouki, T., Bouich, A., Elkouari, Y., Erguig, H., Migalska-Zalas, A., Aissat, A.: InP/InGaAsP thin films based solar cells: Lattice mismatch impact on efficiency. Opt. Mater. **131**, 112704 (2022)
20. Tarbi, A., Chtouki, T., Bouich, A., Elkouari, Y., Erguig, H., Migalska-Zalas, A.: Prediction of mechanical properties of $In_{1-x}$ $Ga_xAs_yP_{1-y}$ lattice-matched to different substrates using artificial neural network (ANN). Adv. Mater. Process. Technol. (2022). https://doi.org/10.1080/2374068X.2022.2118943
21. Alahmary, A., Bouarissa, N., Kamli, A.: Band structure and lattice vibration properties of III-P ternary alloys. Physica B **403**(12), 1990–1995 (2008)
22. Drigo, A.V., Aydinli, A., Carnera, A., Genova, F., Rigo, C., Ferrari, C., ... Salviati, G.: On the mechanisms of strain release in molecular-beam-epitaxy-grown $In_xGa_{1-x}As$/GaAs single heterostructures. J. Appl. Phys. **66**(5), 1975–1983 (1989)
23. Tarbi, A., Chtouki, T., Benahmed, A., Elkouari, Y., Erguig, H., Migalska-Zalas, A.: Transport properties of the deformed quaternary InGaAsP epitaxied on different substrates. Optik **267**, 169657 (2022)
24. Moss, T.S.: Relations between the refractive index and energy gap of semiconductors. Phys. Stat. Sol. (B) **131**(2), 415–427 (1985)

## Authors and Affiliations

**A. Tarbi[1] · T. Chtouki[2] · M. A. Sellam[1] · A. Benahmed[3] · Y. El kouari[1] · H. Erguig[2] · A. Migalska-Zalas[4] · I. Goncharova[5,6] · S. Taboukhat[6] · M. Tlemçani[7,8]**

✉ A. Tarbi
amal_tarbi@yahoo.fr

[1] Laboratory of Condensed Matter and Renewable Energy, Faculty of Sciences and Technology, University Hassan II of Casablanca, BP146, Mohammedia, Morocco

[2] Superior School of Technology, Materials Physics and Subatomic Laboratory, Ibn-Tofail University, PB 242, 14000 Kenitra, Morocco

[3] Faculty of Technology, University of Saad Dahlab Blida.1, Blida, Algeria

[4] Faculty of Science and Technology, Jan Dlugosz University in Czestochowa, Al. Armii Krajowej 13/15, 42201 Czestochowa, Poland

[5] Department of Commodity Science, Safety and Quality Management, State University of Trade and Economics, 19 Kyoto Str., Kiev 02156, Ukraine

[6] University of Angers, LPhiA, SFR MATRIX, 2 Bd. Lavoisier, 49045 Angers, France

[7] Department of Mechatronics Engineering, School of Science and Technology, Universidade de Évora, 7000-671 Évora, Portugal

[8] Instrumentation and Control Laboratory (ICL), Institute of Earth Sciences (ICT), Universidade de Évora, 7000-671 Évora, Portugal